Magnetic field propagation in a two ion species planar plasma opening switch

H. R. Strauss
New York University, New York, New York 10012

R. Doron, R. Arad, B. Rubinstein, and Y. Maron
Weizmann Institute of Science, Rehovot 76100, Israel

A. Fruchtman
Holon Institute of Technology, Holon 58102, Israel

(Received 22 September 2006; accepted 11 April 2007; published online 24 May 2007)

Three fluid plasma evolution equations are applied to the problem of magnetic field propagation in a planar plasma opening switch. For certain initial conditions in which Hall parameter $H \sim 1$, magnetic field penetration due to the Hall field, initially, as expected, either opposes or adds to the hydromagnetic pushing, depending on the polarity of the magnetic field relative to the density gradient. Later, however, the plasma pushing by the magnetic field is found in the case studied here to modify the plasma density in a way that the density gradient tends to align with the magnetic field gradient, effectively turning off the Hall effect. The penetration of the magnetic field then ceases and plasma pushing becomes the dominant process. © *2007 American Institute of Physics*.
[DOI: 10.1063/1.2736353]

I. INTRODUCTION

The mechanism of penetration of a fast-rising magnetic field pulse into a plasma is a fundamental issue in plasma physics. A laboratory application in which this issue is central is the plasma opening switch (POS). In such a system, a pulsed current is conducted through a plasma bridge between two electrodes, before being rapidly switched to a parallel load due to a fast rise in the plasma impedance. Plasma opening switches operating with low density ($<10^{14}$ cm^{-3}), nearly collisionless plasmas have been found to be characterized by a rapid magnetic field penetration that is much faster than expected by collisional diffusion.[1–4] At these low densities, this has been explained by electron magnetohydrodynamic (EMHD) theory,[5–7] according to which the Hall field induces a fast penetration if the scale length of nonuniformity L is much smaller than the ion skin depth c/ω_{pi}, i.e., the Hall parameter H,

$$H \equiv \frac{c}{\omega_{pi} L} = \frac{v_A}{\Omega_i L}, \tag{1}$$

satisfies $H \gg 1$. Here v_A is the hydromagnetic velocity, expressed in the form of Alfvén velocity in which the magnetic field takes its upstream value and the mass density its downstream value, and Ω_i is the ion cyclotron frequency. At the opposite MHD limit, $H \ll 1$, plasma pushing is expected to be dominant.[8]

The evolution of the magnetic field in POS of moderate densities, in which $H \approx 1$, was investigated in recent experiments.[9,10,12] One of the goals of the experiments was to explore which of the two competing processes, plasma pushing or magnetic field penetration, becomes dominant. When $H \approx 1$ the prediction of the magnetic field evolution is harder since, because of the plasma pushing, the density is modified and the value of the Hall parameter H changes in time. In this paper we demonstrate a case in which, as a result of the plasma pushing, the density is modified in such a way that after a certain time the penetration of the magnetic field into the plasma ceases and the plasma pushing remains the dominant process. This is in contrast to cases shown in previous theoretical analyses, in which the penetration did not slow down due to the plasma pushing[8] and was even enhanced by such a pushing.[13]

When there is more than one particle species, as in the moderate density POS, the situation is more complicated. The plasma consists of light and heavy ion species, neutralized by electrons. When $H \sim 1$, the motion consists of MHD, along with drifts perpendicular to the magnetic field. Light and heavy ions drift in opposite directions, parallel or antiparallel to the plasma current.

In this paper, three fluid equations of motion[8,14–16] are applied to the POS. We employ the formulation by Gordeev[14] which decomposes the velocity into a MHD part and a difference velocity between the two ion species.

II. THREE-FLUID EQUATIONS

In the experiment reported in Refs. 9, 10, and 12, there were two ion species, hydrogen ions with density n_i and carbon ions with density n_Z and charge Ze. From quasineutrality (negligible Debye length), the electron density is

$$n_e = n_i + Z n_Z. \tag{2}$$

The electron velocity can be expressed in terms of the current, as

$$n_e \mathbf{v}_e = n_i \mathbf{v}_i + Z n_Z \mathbf{v}_Z - H \nabla \times \mathbf{B}. \tag{3}$$

Here dimensionless variables have been introduced. The magnetic field, density, and length are normalized to typical values. Velocities are expressed in terms of Alfvén speed.

The time is expressed in Alfvén transit times $\tau_A = L/v_A$, where L is the length. The scaling is discussed in Appendix A. Since the experiments of interest have low plasma pressure relative to magnetic pressure, the plasma pressure will be neglected. Neglecting electron inertia, the electron momentum equation is

$$\mathbf{E} + \mathbf{v}_e \times \mathbf{B} = 0 \tag{4}$$

where the electron pressure is neglected. The dimensionless ion momentum equations are,

$$\frac{\partial \mathbf{v}_i}{\partial t} + \mathbf{v}_i \cdot \nabla \mathbf{v}_i = \frac{1}{H}(E + \mathbf{v}_i \times \mathbf{B}), \tag{5}$$

$$\frac{\partial \mathbf{v}_Z}{\partial t} + \mathbf{v}_Z \cdot \nabla \mathbf{v}_Z = \frac{Z}{\mu_Z H}(E + \mathbf{v}_Z \times \mathbf{B}), \tag{6}$$

where μ_Z is the mass ratio m_Z/m_i, and the ion pressure is neglected. The light ion momentum equation (5) can be multiplied by n_i and the heavy ion momentum equation (6) by $\mu_Z n_Z$, and the equations added together with the electron equation to obtain the MHD result, where all the terms are standard except the inertia terms containing $\mathbf{v}_D$,

$$n\frac{\partial \mathbf{v}}{\partial t} + n\mathbf{v} \cdot \nabla \mathbf{v} + \mu_Z \nabla \cdot \left(\frac{n_i n_Z}{n} \mathbf{v}_D \mathbf{v}_D \right) = (\nabla \times \mathbf{B}) \times \mathbf{B} + \mu n \nabla^2 \mathbf{v}. \tag{7}$$

Here μ is a viscosity. More details of the derivation appear in Ref. 14, which also contains a more complete dissipative model than we employ here. The mass density and center of mass velocity have been introduced,

$$n = n_i + \mu_Z n_Z, \tag{8}$$

$$n\mathbf{v} = n_i \mathbf{v}_i + \mu_Z n_Z \mathbf{v}_Z \tag{9}$$

along with the difference velocity

$$\mathbf{v}_D = \mathbf{v}_i - \mathbf{v}_Z. \tag{10}$$

Next, the heavy ion equation (6) can be divided by μ_Z and subtracted from the light ion equation (5) to give

$$\frac{\partial \mathbf{v}_D}{\partial t} = \frac{\Omega}{H}\mathbf{v}_D \times \frac{\mathbf{B}}{B} + \mathbf{F}, \tag{11}$$

where

$$\Omega = \frac{ZnB}{\mu_Z n_e}, \tag{12}$$

$$\mathbf{F} = \frac{\mu_Z - Z}{\mu_Z n_e} \nabla \times \mathbf{B} \times \mathbf{B} - \mathbf{v} \cdot \nabla \mathbf{v}_D - \mathbf{v}_D \cdot \nabla \mathbf{v} - \mu_Z^2 \frac{n_Z \mathbf{v}_D}{n} \cdot \nabla \frac{n_Z \mathbf{v}_D}{n} + \frac{n_i \mathbf{v}_D}{n} \cdot \nabla \frac{n_i \mathbf{v}_D}{n} - \mu \nabla^2 \mathbf{v}_D. \tag{13}$$

The electron velocity (3) can be expressed as

$$\mathbf{v}_e = \mathbf{v} + (\mu_Z - Z)\frac{n_i n_Z}{n n_e}\mathbf{v}_D - \frac{H}{n_e}\nabla \times \mathbf{B}. \tag{14}$$

Using this in the induction equation gives

$$\frac{\partial \mathbf{B}}{\partial t} = \nabla \times \left[\left(\mathbf{v} + (\mu_Z - Z)\frac{n_i n_Z}{n n_e}\mathbf{v}_D - \frac{H}{n_e}\nabla \times \mathbf{B} \right) \times \mathbf{B} - \eta \nabla \times \mathbf{B} \right], \tag{15}$$

where η is the resistivity. The mass density satisfies

$$\frac{\partial n}{\partial t} = -\nabla \cdot (n\mathbf{v}) + \chi \nabla^2 n, \tag{16}$$

where χ is a diffusion coefficient, and the electron density satisfies

$$\frac{\partial n_e}{\partial t} = -\nabla \cdot \left(n_e \mathbf{v} + (\mu_Z - Z)\frac{n_i n_Z}{n}\mathbf{v}_D \right) + \chi \nabla^2 n_e. \tag{17}$$

The ion densities can be obtained from the mass density (8) and electron density (2),

$$n_i = \frac{\mu_Z n_e - Zn}{\mu_Z - Z}, \tag{18}$$

$$n_Z = \frac{n - n_e}{\mu_Z - Z}, \tag{19}$$

and the ion velocities can be obtained from the mass velocity and difference velocity,

$$\mathbf{v}_i = \mathbf{v} + \frac{\mu_Z n_Z}{n}\mathbf{v}_D, \tag{20}$$

$$\mathbf{v}_Z = \mathbf{v} - \frac{n_i}{n}\mathbf{v}_D. \tag{21}$$

There is now a complete set of equations (7), (11), and (15)–(17), for the primary variables $\mathbf{v}$, $\mathbf{v}_D$, $\mathbf{B}$, n, and n_e. The ion densities n_i, n_Z are derived from (18) and (19), and the ion velocities from (20) and (21).

The first term on the right-hand side of (11) causes the velocity to rotate with angular frequency Ω/H. The other terms correspond to inertial and Lorentz acceleration. The rotation effect appears to be important in making a transition to MHD behavior in a dense planar plasma opening switch. After an initial transient involving rotation, $\mathbf{v}_D$ becomes a drift aligned with the current. In steady state, from (11), neglecting pressure and inertial terms,

$$\mathbf{v}_D \approx -H\frac{(\mu_Z - Z)}{Zn}\nabla \times \mathbf{B}. \tag{22}$$

The drift is in the direction of the plasma current.

III. SIMULATION OF A PLANAR PLASMA OPENING SWITCH

In this section we show simulations of a model planar plasma opening switch using the equations developed in the previous section. The simulations were done with a substantially modified version of the M3D (Refs. 17 and 18) code. In the experiments, collisional dissipation is expected to be small compared to turbulent dissipation. In particular, according to the commonly used Spitzer approach ion-ion col-

lisions are evidently negligible. Ions ejected from the flashboard plasma source[11] used in this experiment have a velocity distribution that corresponds to an effective ion temperature greater than 50 eV. Under these conditions the ion-ion collision frequency is of the order 4×10^6 s^{-1}; namely, the time interval between collisions is of the order of the entire experiment duration (300 ns). Possibly, there are other mechanisms that may enhance collision frequency, but these are not dealt in this work. It is a common practice to use fluid equations to simulate collisionless or nearly collisionless plasma. This is often done in magnetic fusion. It is also done in several theoretical studies[5,8,13,15] relevant to the plasma opening switch problem.

Because of numerical difficulties with low density, the problem of field penetration from a vacuum region into the plasma is not considered here. It is assumed that the field has penetrated into the plasma. The computations are concerned with the propagation of the magnetic field in the plasma. The computations used a 50×100 rectangular mesh. The dimensionless radial width is $L_x=2.4L$, and the vertical length is $L_y=5L$, similar to the experiments.[9,10,12] Dissipation is added to the equations; the viscosity had the same magnitude as resistivity, $\mu=\eta=2.5\times10^{-2}v_AL$. Rather than using collisional diffusion coefficients,[14] the values of η,μ are compatible with anomalous microturbulent diffusion in the experiments.[9,10,12] A small diffusion term was added to the density equations, with $\chi=10^{-3}v_AL$, in order to provide some numerical smoothing.

The magnetic field, and electron density are shown in Figs. 1(a) and 1(d) at time $t=0$. The light ion (proton) density and the heavy ion density have a linear dependence on x of the form $n_0(1+3x/L)$, where n_0 is either n_{i0} or n_{Z0}. The charge of the heavy ions (carbon) is $Z=4$, and the heavy ion mass is $\mu_Z=12$. The normalized $n_{i0}=1$, and the normalized $n_{Z0}=1/Z$. The magnetic field B has only a z component. The initial magnetic field is of the form $B=[1-y/(0.4L)]^4B_0$ for $y<0.4L$, and $B=0$ for $y\geq0.4L$. These initial conditions are thought to be consistent with the experiment. The initial velocity of the ion species is zero. In the experiment, the ion axial velocities from the source are small compared to the MHD and Hall velocities.

With the finite element method employed here, there is no need to specify boundary conditions, except for the diffusion terms. For these terms, Neumann (zero normal derivative) boundary conditions are used, except for the magnetic field at $y=0$. There, the magnetic field is held constant in time, $B(x,0,t)=1$. The small diffusion of the densities has little effect on the density gradient. It does not cause sufficient relaxation of the density gradient to produce the effects reported below.

The drift equation (11) appears singular in the limit $H\rightarrow0$. An implicit time integration method for small H is given in Appendix B.

In the following simulations the normalized Hall parameter $H=2$.

Contour plots of the magnetic field and electron density are shown in Fig. 1. Shown are (a) the initial magnetic field and (d) the initial electron density. Figure 1(b) shows the magnetic field at time $t=7.3\tau_A$. The front has advanced into the plasma. The corresponding electron density is shown in Fig. 1(e). The electron density has piled up at the front. The electron density contours are aligned with the magnetic field front, although they are not aligned behind and ahead of the front. This implies that in the magnetic front, the Hall velocity is small. This will be verified below. Figure 1(c) shows the magnetic field at time $t=14.1\tau_A$, at which time the front has almost reached the end boundary. The field has advanced somewhat further on the left, lower density side. Figure 1(f) shows n_e at the same time. The contours are aligned with the magnetic front, but there is also a high density blob on the high initial density side, behind the front.

The time evolution of the magnetic field in the midplane $x=L_x/2$ is shown in Fig. 2. The magnetic field as a function of y is shown at equal time intervals $2\tau_A$. The magnetic field front advances at a uniform rate in a self similar manner at later time intervals.

The next set of figures depict the case of opposite polarity, in which the sign of B is negative. The plots are of $|B|$. The initial B in (a) has the same magnitude as in Fig. 1(a), but with opposite sign, and the electron density (d) is the same as in Fig. 1(d). The initial densities are the same as in the previous case.

Figure 3(b) shows the magnetic field at time $t=6.9\tau_A$. Here the magnetic front has not advanced as far as in Fig. 1(b). The corresponding electron density is shown in Fig. 3(e). The electron density contours are aligned with the magnetic field front, although they are not aligned behind and ahead of the front. The magnetic field in Fig. 3(c) at $t=14.4\tau_A$ likewise has advanced less than in Fig. 1(c). The electron density is aligned with the magnetic front in Fig. 3(f) at the same time. Behind the front is a density blob similar to Fig. 1(f), but more aligned with the magnetic field.

The magnetic field as a function of y in the midplane is shown at equal time intervals in Fig. 4. At early times, the contours are close together. The front moves backwards slightly, but then it picks up speed in the positive y direction.

The two cases of positive and negative polarity are compared in Fig. 5, which shows the magnetic front velocity as a function of time. The front position y_B is defined as that value of y at which $|J_x|$ is a maximum, in the midplane $x=L_x/2$, where

$$J_x=\frac{\partial B}{\partial y}. \tag{23}$$

After a certain period of time, the two velocities asymptote to almost the same value, which is approximately the Alfvén velocity in the front, as will be shown in the following.

The Hall velocity can be defined

$$\mathbf{v}_H=-HB\,\nabla\left(\frac{1}{n_e}\right)\times\hat{z}, \tag{24}$$

where $\hat{z}$ is the unit vector in the z direction. Initially $\mathbf{v}_H$

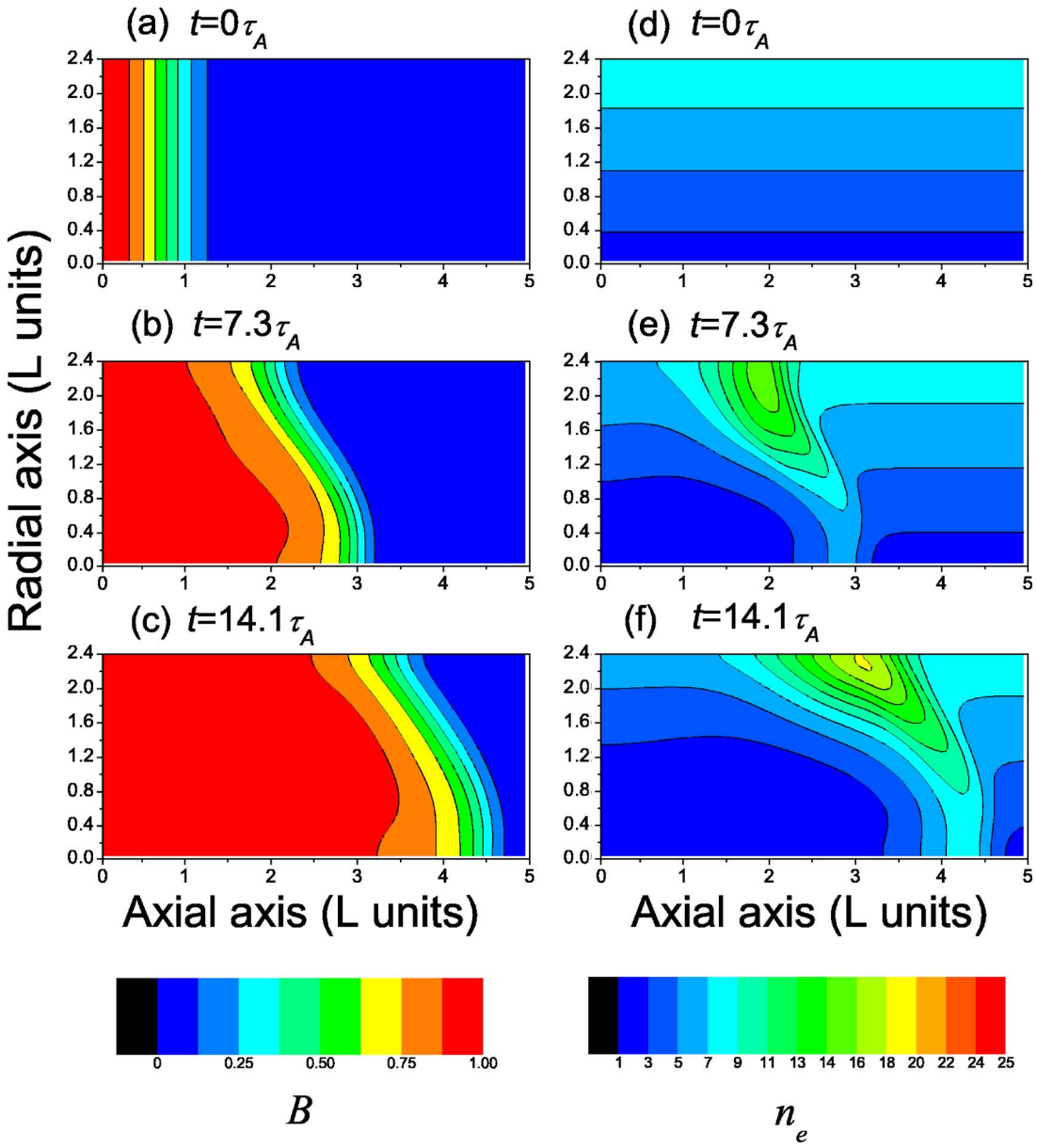

FIG. 1. (Color online) (a), (b), (c) Magnetic field evolution, for $H=2$ and positive polarity. Contours of $|B|$ are plotted. (d), (e), (f) Electron density n_e evolution at the same times. B and n_e are in dimensionless units.

points in the $\pm y$ direction, but it rotates into the $\pm x$ direction. The magnetic field gradient causes $\mathbf{v}$ to accelerate in the axial, y direction. In turn this causes the density to pile up, so the density gradient there is predominantly in the y direction. Second, the difference velocity, initially in the y direction, rotates into the x direction with angular frequency Ω/H. Having rotated, it relaxes the density gradients in the magnetic front. However, the density pileup appears to be the dominant effect.

It was pointed out in Ref. 14 that in the limit $\mu_Z \gg Z$, the difference velocity v_D, in the event of neglecting the inertial term, may be of the order of v_H, which can essentially change the magnetic field evolution (14) and (15). Since the literature has emphasized v_H, we will consider v_H and v_D separately.

The Alfvén velocity and Hall velocity in the magnetic

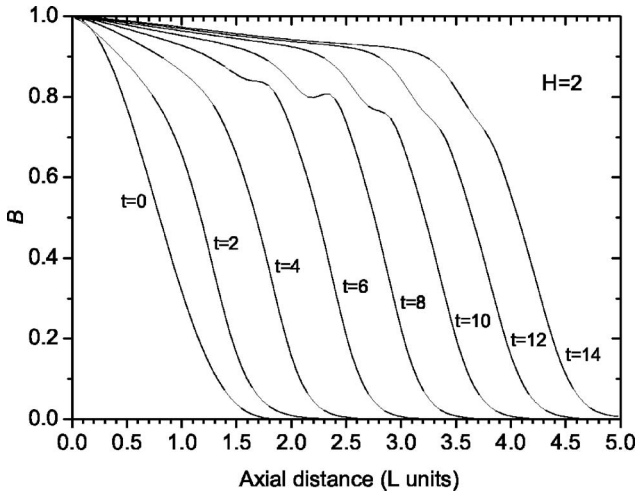

FIG. 2. Magnetic field as a function of axial distance y at equal time intervals, for positive polarity and $H=2$.

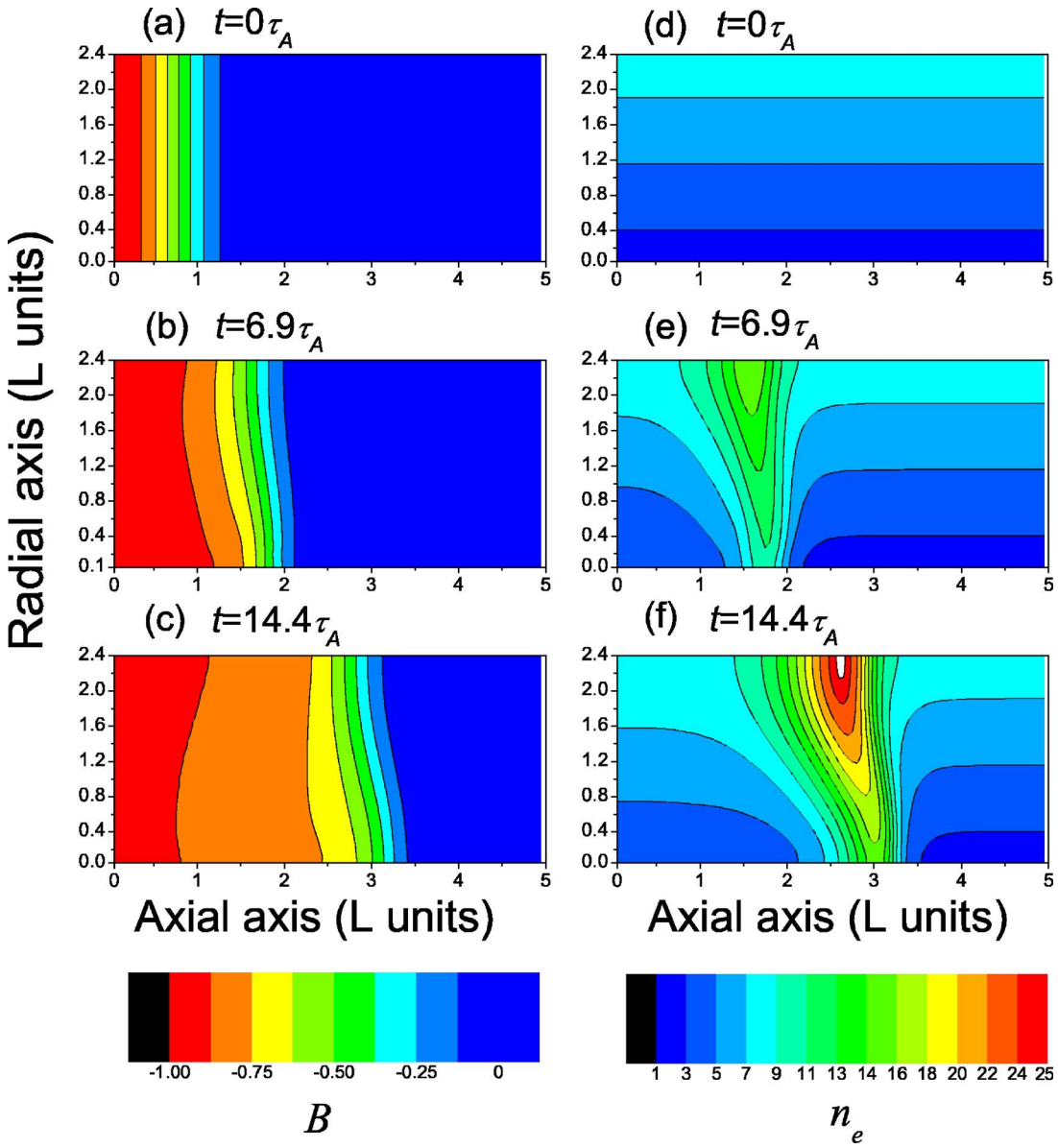

FIG. 3. (Color online) (a), (b) (c) Magnetic field evolution, for $H=2$ and negative polarity. Contours of $|B|$ are plotted. (d), (e), (f) Electron density at evolution at the same times. Contour levels are the same as in Fig. 1.

front are compared in Fig. 6. The plots show two quantities. We define

$$v_{Af} = L\left\langle \frac{|J_x|}{\sqrt{n}} \right\rangle \tag{25}$$

using (23). The average over the front is defined as

$$\langle f \rangle = \frac{\int f J_x dxdy}{\int J_x dxdy}, \tag{26}$$

where f is the quantity to be averaged. This weighting is used because J_x is large only in the magnetic front. The quantity v_{Af} is a measure of the magnetic pushing force (7) in the front and is comparable in magnitude to an average Alfvén velocity in the front. We also define

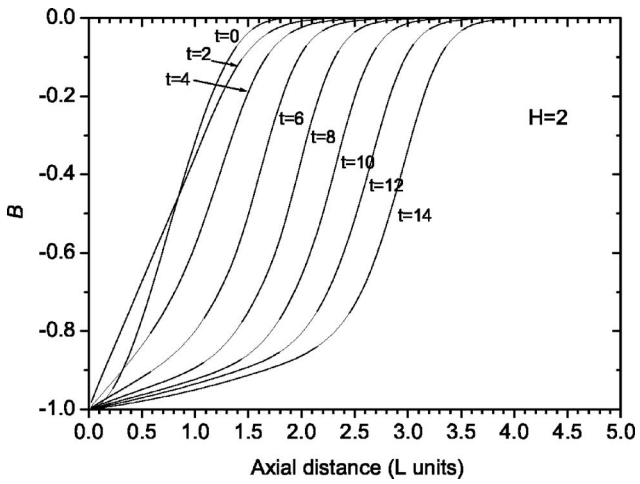

FIG. 4. Magnetic field as a function of axial distance y at equal time intervals, for negative polarity and $H=2$.

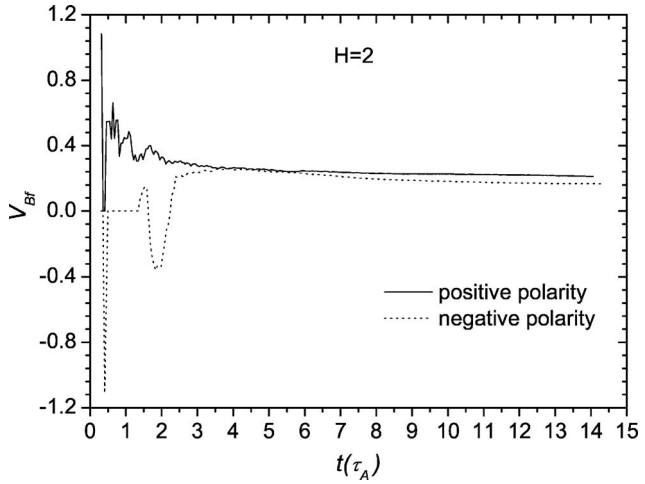

FIG. 5. Magnetic front velocity as a function of time for the two polarities with $H=2$. After an initial transient, both cases asymptote to almost the same front velocity.

$$v_{Hf} = L\left\langle \left| \mathbf{v}_H \cdot \frac{\nabla B}{B} \right| \right\rangle \tag{27}$$

using (24), which measures the strength of the Hall term (15). In Fig. 6, v_{Af} and v_{Hf} are shown as a function of time for positive and negative polarity. It can be seen that v_{Af} is comparable in the two cases, and is comparable to the front velocity shown in Fig. 5. Initially v_{Hf} is also comparable to v_{Af} for both polarities, but it decays toward zero. This quantifies the observations made above that the magnetic field penetration ceases, as the electron density and the magnetic field become aligned in the magnetic front. We have chosen $H=2$ and the initial density gradients in order to make the Hall term initially comparable to the Alfvén term. We see that it has an effect on the magnetic field evolution for only a certain period of time. After a time delay, the magnetic front propagates at the same speed for both polarities.

There is also the question of the role of three fluids on the magnetic field propagation. The difference velocity v_D is

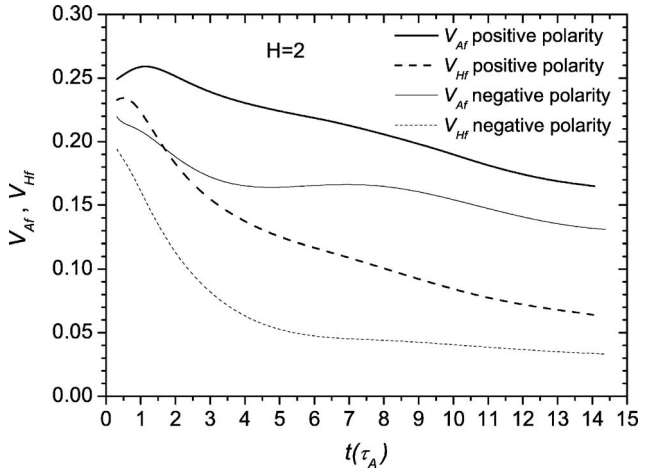

FIG. 6. Alfvén and Hall velocity in the front as a function of time for the two polarities with $H=2$. Initially the Alfvén and Hall velocities are comparable, but the Hall velocity tends to zero. The front velocity is close to the Alfvén velocity.

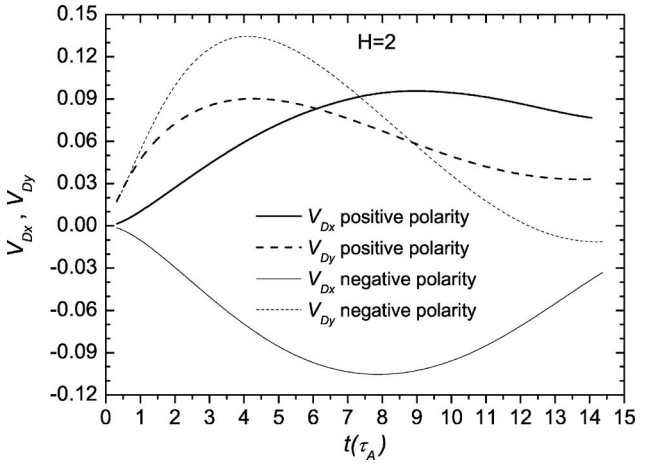

FIG. 7. Components of difference velocity v_D in the front as a function of time for the two polarities with $H=2$. At later times, $|v_{Dy}|<|v_{Dx}|$ for both polarities, and $|v_{Dy}|<|v_A|$ for both polarities.

relatively small compared to the Alfvén velocity, and tends to align with the magnetic field, as noted in (22). Figure 7 shows components of the difference velocity v_D in the front as a function of time for two cases with $H=2$. The velocity components are averaged in the magnetic front as in (26) $\langle v_{Dx}\rangle$, $\langle v_{Dy}\rangle$. At later times, $|\langle v_{Dy}\rangle|<|\langle v_{Dx}\rangle|$ for both polarities, and $|\langle v_{Dy}\rangle|<|v_{Af}|$ for both polarities. Hence the drift velocity tends to align with the magnetic front and becomes unimportant for magnetic field propagation. However, it has an effect on the density evolution. Comparing Fig. 1(f) and Fig. 3(f), the electron density blob appears to be moving in different directions along the magnetic field front. From (17) the electron density evolution depends on $\mathbf{v}$, which is predominantly in the axial, $\hat{y}$ direction, and the difference velocity $\mathbf{v}_D$, which is predominantly in the $\hat{x}$ direction and depends on the sign of the magnetic field. We see from Figs. 5 and 7 that in the case presented here, v_H is somewhat larger than v_D, and that both of the these velocities tend to align with the magnetic field.

We have done the simulations with three fluids because of the experimental conditions, but in fact the results are qualitatively similar when $v_D=0$. In the two fluid case also, the Hall effect is important for a only finite time, after which plasma pushing is dominant.

For smaller H, the tendency for the Hall effect to be suppressed is even more dominant. This is illustrated in Fig. 8, which shows the magnetic front velocity as a function of time for both polarities, for $H=1$. The agreement between the front velocity for the two polarities is even closer than in Fig. 5.

IV. CONCLUSION

In this paper we have applied three fluid plasma evolution equations to the problem of magnetic field propagation in a planar plasma opening switch. We find that there is a tendency for the Hall effect to be suppressed, for Hall parameter $H\sim 1$. Initially the Hall velocity either opposes or adds to the Alfvén velocity, depending on the polarity of the magnetic field, allowing fast magnetic field penetration. Be-

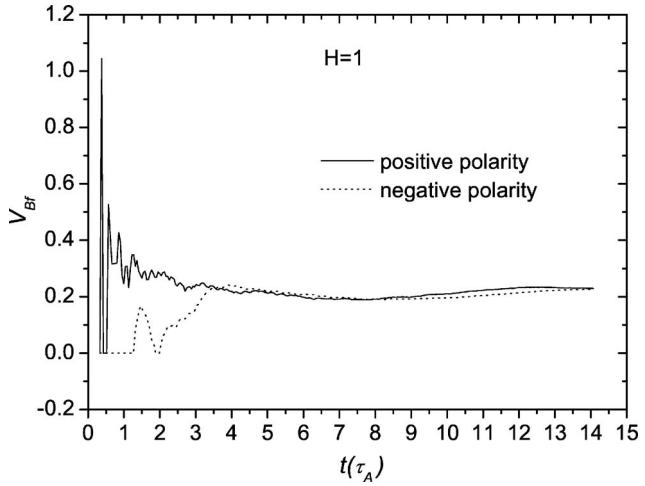

FIG. 8. Magnetic front velocity as a function of time for the two polarities with $H=1$. After an initial transient, both cases asymptote to the same front velocity.

cause the density is compressed by the fluid velocity, which is independent of the Hall velocity, the electron density gradient tends to align with the magnetic field gradient, effectively turning off the Hall effect. Thereafter the plasma pushing is the dominant process. The calculation of the time period in which the magnetic field penetration is important, before it ceases due to the pushing, will be calculated in a future study. This paper shows that the observed magnetic field penetration is not always easily explained even by the Hall field. Specular reflection of the light-ion species, observed in the experiment[9,10] might affect the plasma penetration. To some extent, this reflection may be modeled by the relative velocity v_D of the two species, but the fluid model cannot account for partial reflection within the light-ion species. There could be additional effects which could alter the competition between plasma pushing and Hall-field induced penetration.

ACKNOWLEDGMENT

This work was supported in part by the U.S. DOE and by the United States-Israel Binational Science Foundation (BSF) Grant No. 2002187.

APPENDIX A: SCALING OF THE EQUATIONS

In cgs units, the ion momentum equation is, after eliminating the electric field with the electron momentum equation,

$$\frac{\partial \mathbf{v}_i}{\partial t} + \mathbf{v}_i \cdot \nabla \mathbf{v}_i = \frac{e}{M_i c}(\mathbf{v}_i - \mathbf{v}_e) \times \mathbf{B}.$$

Normalize $\tilde{t}=t/\tau_A$, where $\tau_A=L/v_A$, and L is the length. The Alfvén velocity is $B_0(4\pi\mu_0 n_0 M_i)^{-1/2}$, where B_0 is a typical value of magnetic field strength, M_i is the light ion mass, and n_0 is a typical ion density. Lengths are normalized to L, so that $\tilde{\nabla}=L\nabla$. The magnetic field is normalized to B_0; $\tilde{\mathbf{B}}=B_0^{-1}\mathbf{B}$. The densities n_a are normalized to n_0, with $\tilde{n_a}=n_0^{-1}n_a$. The velocities are normalized to v_A, with $\tilde{\mathbf{v}}_a=v_A^{-1}\mathbf{v}_a$. The pressure is normalized to $\tilde{p}=4\pi\mu_0 p/B_0^2$. Finally

$$H = \frac{v_A M_i c}{eB_0 L} = \frac{cM_i^{1/2}}{L(4\pi n_0)^{1/2} e}.$$

In dimensionless units,

$$\frac{\partial \tilde{\mathbf{v}}_i}{\partial \tilde{t}} + \tilde{\mathbf{v}}_i \cdot \tilde{\nabla}\tilde{\mathbf{v}}_i = \frac{1}{H}(\tilde{\mathbf{v}}_i - \tilde{\mathbf{v}}_e) \times \tilde{\mathbf{B}} - \frac{\tilde{\nabla}\tilde{p}_i}{\tilde{n}_i}.$$

The electron velocity can be expressed in terms of the current, as

$$n_e \mathbf{v}_e = n_i \mathbf{v}_i + Z n_Z \mathbf{v}_Z - \frac{c}{4\pi\mu_0 e} \nabla \times \mathbf{B}.$$

Using the normalizations gives

$$\frac{1}{H}(\tilde{n_e}\tilde{\mathbf{v}}_e - \tilde{n_i}\tilde{\mathbf{v}}_i - Z\tilde{n_Z}\tilde{\mathbf{v}}_Z) = \tilde{\nabla} \times \tilde{\mathbf{B}}.$$

The dimensionless induction equation is

$$\frac{\partial \tilde{\mathbf{B}}}{\partial \tilde{t}} = \tilde{\nabla} \times (\tilde{\mathbf{v}}_e \times \tilde{\mathbf{B}}).$$

APPENDIX B: IMPLICIT METHOD FOR DRIFT

The drift equation (11) appears singular in the limit $H \to 0$. This suggests an implicit numerical approach. Discretizing in time, (11) becomes

$$\mathbf{v}_D^{n+1} - dt\frac{\Omega}{H}\mathbf{v}_D^{n+1} \times \frac{\mathbf{B}}{B} = \mathbf{v}_D^n + dt\mathbf{F},$$

where $\mathbf{v}_D^{n+1}$ refers to time level $n+1$, dt is the time step, and all other quantities are assumed at time level n. This can be inverted in the form

$$\mathbf{v}_D^{n+1} = \frac{H}{H^2 + dt^2\Omega^2}\left(H(\mathbf{v}_D^n + dt\mathbf{F}) + dt\Omega(\mathbf{v}_D^n + dt\mathbf{F}) \times \frac{\mathbf{B}}{B}\right).$$

If $H=0$, the solution is $\mathbf{v}_D=0$.

[1] B. V. Weber, R. J. Commisso, R. A. Meger, J. M. Neri, W. F. Oliphant, and P. F. Ottinger, Appl. Phys. Lett. **45**, 1043 (1984).
[2] M. Sarfaty, Y. Maron, Ya. E. Krasik, A. Weingarten, R. Arad, R. Shpitalnik, A. Fruchtman, and S. Alexiou, Phys. Plasmas **2**, 2122 (1995).
[3] R. Shpitalnik, A. Weingarten, K. Gomberoff, Ya. Krasik, and Y. Maron, Phys. Plasmas **5**, 792 (1998).
[4] A. Weingarten, R. Arad, Y. Maron, and A. Fruchtman, Phys. Rev. Lett. **87**, 115004 (2001).
[5] A. Fruchtman, Phys. Fluids B **3**, 1908 (1991).
[6] A. S. Kingsep, Yu. V. Mohkov, and K. V. Chukbar, Sov. J. Plasma Phys. **10**, 495 (1984); A. S. Kingsep, K. V. Chukbar, and V. V. Yankov, in *Reviews of Plasma Physics*, edited by B. Kadomstev (Consultants Bureau, New York, 1990), Vol. 16, p. 243.
[7] A. V. Gordeev, A. S. Kingsep, and L. I. Rudakov, Phys. Rep. **243**, 215 (1994).
[8] A. Fruchtman, Phys. Fluids A **4**, 855 (1992).
[9] R. Arad, K. Tsigutkin, Y. Maron, A. Fruchtman, and J. D. Huba, Phys. Plasmas **10**, 112 (2003).
[10] R. Arad, K. Tsigutkin, Y. Maron, and A. Fruchtman, Phys. Plasmas **11**, 112 (2003).
[11] R. Arad, K. Tsigutkin, Yu. V. Ralchenko, and Y. Maron, Phys. Plasmas **7**, 3797 (2000).

[12]R. Doron, R. Arad, K. Tsigutkin, A. Weingarten, A. Starobinets, V. A. Bernshtam, E. Stambulchik, Yu. V. Ralchenko, Y. Maron, A. Fructman, A. Fisher, J. D. Huba, and M. Roth, Phys. Plasmas **11**, 2411 (2004).
[13]A. Fruchtman and L. I. Rudakov, Phys. Rev. Lett. **69**, 2070 (1992); Phys. Rev. E **50**, 2997 (1994).
[14]A. V. Gordeev, Plasma Phys. Rep. **27**, 659 (2001); translated from Fiz. Plazmy **27**, 700 (2001).
[15]N. Chakrabarti, A. Fruchtman R. Arad, and Y. Maron, Phys. Lett. A **297**, 92 (2002).
[16]M. A. Shay and M. Swisdak, Phys. Rev. Lett. **93**, 275001 (2004).
[17]W. Park, E. V. Belova, G. Y. Fu, X. Tang, H. R. Strauss, and L. E. Sugiyama, Phys. Plasmas **6**, 1796 (1999).
[18]L. E. Sugiyama and W. Park, Phys. Plasmas **7**, 4644 (2000).